Biochemical and Biophysical Research Communications 446 (2014) 1079–1084

Contents lists available at ScienceDirect

Biochemical and Biophysical Research Communications

journal homepage: www.elsevier.com/locate/ybbrc

A mouse model of mitochondrial complex III dysfunction induced by myxothiazol

Mina Davoudi [a], Jukka Kallijärvi [b], Sanna Marjavaara [b], Heike Kotarsky [a], Eva Hansson [a], Per Levéen [a,b], Vineta Fellman [a,b,c,*]

[a] Pediatrics, Department of Clinical Sciences, Lund, Lund University, Lund 22185, Sweden
[b] Folkhälsan Research Center, Biomedicum Helsinki, University of Helsinki, 00014, Finland
[c] Children's Hospital, Helsinki University Hospital, University of Helsinki, Helsinki 00029, Finland

ARTICLE INFO

Article history:
Received 13 March 2014
Available online 21 March 2014

Keywords:
Respiratory chain complex III
Chemical inhibition of complex III
Mitochondria
Experimental hepatopathy
BCS1L
Mouse model

ABSTRACT

Myxothiazol is a respiratory chain complex III (CIII) inhibitor that binds to the ubiquinol oxidation site Qo of CIII. It blocks electron transfer from ubiquinol to cytochrome *b* and thus inhibits CIII activity. It has been utilized as a tool in studies of respiratory chain function in *in vitro* and cell culture models. We developed a mouse model of biochemically induced and reversible CIII inhibition using myxothiazol. We administered myxothiazol intraperitoneally at a dose of 0.56 mg/kg to C57Bl/J6 mice every 24 h and assessed CIII activity, histology, lipid content, supercomplex formation, and gene expression in the livers of the mice. A reversible CIII activity decrease to 50% of control value occurred at 2 h post-injection. At 74 h only minor histological changes in the liver were found, supercomplex formation was preserved and no significant changes in the expression of genes indicating hepatotoxicity or inflammation were found. Thus, myxothiazol-induced CIII inhibition can be induced in mice for four days in a row without overt hepatotoxicity or lethality. This model could be utilized in further studies of respiratory chain function and pharmacological approaches to mitochondrial hepatopathies.

1. Introduction

Mitochondrial complex III (CIII, cytochrome *bc*1 EC 1.10.2.2.) consists of 11 subunits present in a dimer formation, in which two Rieske iron sulfur protein (RISP) subunits form the catalytic center. CIII has a central role in the respiratory chain electron transfer from ubiquinol into its subunit cytochrome *b*, followed by the RISP-dependent transfer from coenzyme Q to cytochrome *c*. Electrons are then transferred to mitochondrial complex IV (CIV) and molecular oxygen.

Two types of CIII inhibitors have been characterized; those targeting the ubiquinol oxidation site in CIII Qo called class I inhibitors (including myxothiazol and stigmatellin), and those binding to the Qi site, class II inhibitors (e.g. antimycin A) [1]. Myxothiazol binds to the proximal domain of Qo site with high affinity and thereby blocks electron transfer from ubiquinol to cytochrome *b* and inhibits CIII activity [2–4]. This inhibitory effect has been used in experimental studies (mainly cell culture models) to investigate CIII dysfunction [5]. Myxothiazol was used in a mouse model of inflammatory responses [6], in which acute lung injury was induced by lipopolysaccharide (LPS) injection and the effect of CIII inhibitors on neutrophil activation investigated. Proinflammatory cytokines induced by LPS were decreased by the administration of myxothiazol, thereby diminishing the severity of LPS inflammation. This was ascribed to the increased H_2O_2 production induced by CIII inhibition [6].

CIII assembly is a multistep process in which at least five known assembly factors or chaperones participate. Of these UQCC1/UQCC2 and TTC19 are responsible for an early assembly stage and BCS1L for the last step, in which RISP is incorporated [7–9].

Several human mitochondrial disorders are caused by genes associated with CIII function and often present with neonatal hepatopathy [10]. Numerous CIII deficiency-causing mutations have been found in the gene encoding the assembly factor BCS1L. These mutations result in decreased incorporation of RISP into CIII and thereby diminished CIII activity [11–15]. Different *BCS1L* mutations present with a variety of phenotypes. A homozygous c.232A > G

Abbreviations: BNGE, blue native gel electrophoresis; CI, complex I; CIII, complex III; CIV, complex IV; HE, hematoxylin–eosin; ip, intraperitoneally; LPS, lipopolysaccharide; RISP, Rieske iron-sulfur protein.

* Corresponding author at: Lasarettsgatan 40, Se-22185 Lund, Sweden. Fax: +46 46 222 07 48.
E-mail address: Vineta.Fellman@med.lu.se (V. Fellman).

http://dx.doi.org/10.1016/j.bbrc.2014.03.058
0006-291X/

mutation causes the most severe phenotype, the GRACILE syndrome, with a distinct neonatal liver disorder and associated clinical findings including fetal growth restriction, Fanconi type amino aciduria, cholestasis, iron overload, lactic acidosis, and early death [15–17]. Other homozygous and compound heterozygous mutations located adjacent to the GRACILE mutation in *BCS1L* cause GRACILE-like diseases [10]. When introduced into the mouse genome the c.232A > G homozygous GRACILE mutation causes a decreased RISP incorporation into CIII and fatal liver disease mimicking the human disorder [18]. Whether the phenotypes in patients with *BCS1L* mutations and in the GRACILE mouse model are caused primarily by decreased CIII function, or if an as yet unknown function of BCS1L plays a role, is not known. To shed light on this question we set out to reversibly inhibit CIII *in vivo* using myxothiazol.

2. Materials and methods

2.1. Animal experiments

The animal experiments were performed with the approval of the Research Animal Ethics Committee of Southern Finland (ESAVI-2010-07284/Ym-23). Wild type C57Bl/J6 mice of 5–6 weeks age (weighing 16–19 g) were studied. The animals were fed with Harlan 2918 Teklad Global 18% Protein Rodent Diet and water ad libitum in a vivarium with 12 h light/dark cycles at room temperature. Animals were randomized to receive myxothiazol or vehicle intraperitoneally (ip).

Myxothiazol dry substance extracted from mycobacteria was received as a kind gift from Professor Dr. Rolf Muller, Helmholtz-Center for Infection Research, Braunschweig, Germany. As myxothiazol is poorly soluble in water, it was diluted in 10% DMSO in saline to a concentration of 25 μg/ml. To avoid toxicity, the dose of myxothiazol was modified from a previous study using 0.5–1 mg/kg [6]. We assessed dose–response for 4 doses (1, 0.75, 0.625, and 0.5 mg/kg) and accordingly chose for the repeated dose 0.56 mg/kg body mass. The myxothiazol solution (200 μl per mouse) was injected ip in the morning with 24 h intervals for at most 4 times (0, 24, 48, and 72 h). Animals (3 per group) were sacrificed by cervical dislocation at time points 24, 26, 48, 50, 72, and 74 h to investigate the effect of a prolonged intervention (24–72) as well as the 2 h response after each injection (Fig. 1). Control mice (3 per group) were given 10% DMSO in saline at identical time points and sacrificed for tissue harvesting similarly as the mice in the intervention group. The mice were observed for any signs of disease, such as lethargy or weight loss during the entire study period from the first injection. Immediately after cervical dislocation liver tissue was collected for histology, mitochondrial isolation, and snap freezing for mRNA extraction and lipid analysis.

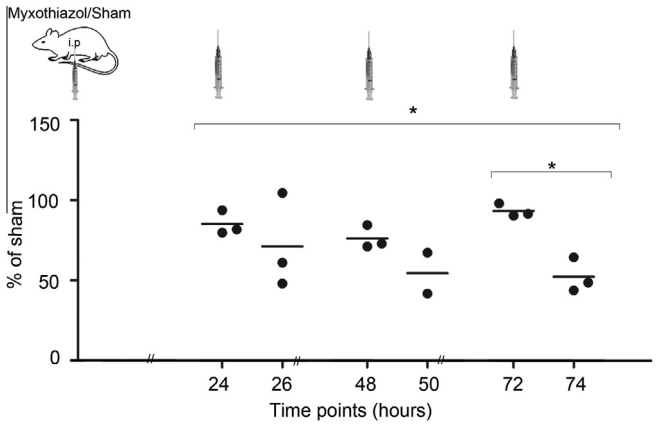

Fig. 1. CIII activity in liver mitochondria of mice receiving 1–4 doses of myxothiazol (0.56 mg/kg i.p) in saline/DMSO or only saline/DMSO (Sham). Injection time points are indicated. Data are presented as percentage of paired sham-treated animals at each time-point ($n = 3$). $^{*}p < 0.05$.

2.2. Isolation of mitochondria from mouse liver

Liver mitochondria were isolated as previously described [18]. Liver tissue samples were kept in ice-cold isolation buffer (320 mM Sucrose, 10 mM Trizma Base, 2 mM EGTA) and homogenized in 2 ml isolation buffer supplemented with 0.1% BSA. The homogenate was subsequently serially centrifuged using the protocol that included a density purification in 19% Percoll (GE Healthcare, Uppsala, Sweden), to obtain a crude mitochondrial pellet. Mitochondrial protein concentration was measured as protein absorbance at 280 nm on a Nanodrop (Fisher Scientific, Vantaa, Finland NanoDrop products, Wilmington, USA).

2.3. Determination of CIII activity

Frozen mitochondrial pellets were resuspended in ice-cold PBS (2 μg/μl). Five microliters of the suspension were added to 650 μl reaction buffer (EDTA 100 μM, 0.2% fatty acid free BSA, 150 μM Cytochrome *C*, 50 mM mono potassium phosphate pH 7.4) pre-warmed at 30 °C. Then 200 μl of mitochondria mix (samples and controls) were placed in triplicates into a pre-warmed 96-well plate, incubated for 5 min at 30 °C in a spectrophotometer (Victor^3 1420 multi label counter, Perkin Elmer Massachusetts, USA). Then 2 μl of decylubiquinol (10 mM in ethanol) were added to each reaction well and the measurement was started after 1 s stirring with an interval of 10–15 s/well in 5 min at 550 nm [18].

2.4. Histology

Liver tissue samples were fixed in 4% buffered formalin. The samples were used for routine hematoxylin–eosin (HE) staining and for staining with periodic acid-Schiff (PAS) without and with diastase for detection of glycogen content. The histological stainings were performed at The Finnish Centre for Laboratory Animal Pathology, Helsinki, Finland.

2.5. Triglyceride quantitation

Triglyceride determinations were performed at time point 74 h from snap-frozen liver tissue samples with an enzymatic method at the National Institute for Health and Welfare, Helsinki, Finland. Hepatic lipids were extracted with the method of Folch et al. [19] and triglycerides were measured as glycerol after chloroform–methanol extraction and hydrolysis. Briefly, liver tissue samples (approximately 50–100 mg) were homogenized via sonication in 1 ml of 95% methanol and mixed with 2 ml of chloroform. The organic phase was further treated with physiological saline and dried under nitrogen. The residual lipid material was dissolved in 200 μl of tetraethylammoniumhydroxide (diluted 1:28 with 95% ethanol) and incubated at 60 °C for 30 min in the presence of 200 μl of 0.05 M HCl. The generated glycerol was measured enzymatically with a triglyceride analysis kit (GPO–PAP 1488872, Roche Diagnostics, Switzerland).

2.6. RNA preparation and quantitative PCR

Total RNA was extracted from frozen liver tissue (obtained at time point 74 h) with Trizol reagent (LifeTechnologies). The RNA was DNAse-treated and cDNA prepared using standard protocols. Levels of selected transcripts were quantified with SYBR Green

method on a CFX96 thermal cycler (Bio-Rad). Expression levels were normalized to β-actin or Gak (cyclin G-associated kinase). Two groups of genes were studied; CIII components or chaperones *Uqcrfs1* (encoding RISP), or *Uqcrc1* (encoding subunit core I of CIII) and *Bcs1l*, and hepatotoxicity/inflammation-associated genes liver glycogen phosphorylase (*Pygl*), thioredoxin reductase *Txnrd1*, flavin-containing mono-oxygenase 1 (*Fmo1*), ATP-binding cassette subfamily B member 11 (*Abcb11/Bsep*) [20] and *Tgf-β* [21]. All primers were ordered from Oligomer (Helsinki, Finland).

2.7. Isolation of respiratory chain complexes and supercomplexes

Frozen mitochondrial pellets were re-suspended in phosphate buffered saline (PBS) including Complete Mini Protease Inhibitor (Roche Diagnostics Scandinavia AB, Stockholm, Sweden). Mitochondrial protein concentrations were measured with the Nanodrop. The samples were pelleted for 5 min at 5000 g and suspended to a concentration of 5 mg/ml in MB2 buffer (1.75 M aminocaproic acid, 75 mM Bis–Tris pH 7.0, + 2 mM EDTA pH 8.0). Mitochondrial membrane proteins were solubilized by incubation with 0.8% digitonin (Sigma Aldrich, Stockholm, Sweden) for 5 min on ice. Samples were centrifuged for 30 min at 13000 g, the supernatant was collected and the protein concentration measured as before. SBG (750 mM aminocaproic acid, 5% Serva Blue G from SERVA Electrophoresis GmbH, Heidelberg, Germany) was added to a final concentration of 4.5% and the samples were stored at −80 °C.

2.8. Blue native gel electrophoresis (BNGE), SDS–PAGE, 2- dimensional BNGE/SDS PAGE and Western blot

Mitochondrial membrane proteins (3 μg/sample) were run on 4–16% blue native gel (Invitrogen, Carlsbad, CA, USA) or 10% SDS gel and blotted onto polyvinylidine difluoride membrane using Iblot™ dry equipment (Invitrogen, Carlsbad, CA, USA). For 2D BNGE/SDS samples were run on BNGE (first dimension), each lane was cut, incubated in 1% β-mercaptoethanol +1% SDS, and overlaid on 10% SDS–PAGE for a second dimension run [22]. Proteins were blotted onto membranes (polyvinylidine difluoride) using Iblot™ dry equipment (Invitrogen, Carlsbad CA, USA). The membranes were blocked with PBS including 0.05% Tween 20 and 5% milk for subsequent antibody incubation. The following antibodies directed to mitochondrial membrane proteins were obtained from MitoSciences (Eugene, Oregon, USA): subunit NDUFA9 (MS111) for detection of complex I (CI), subunit Rieske (MS305) and subunit Core1 (MS303) for CIII, and CIV subunit I (MS404) for detection of CIV, as well as Porin (MSA05). The antibody against NDUFV1 subunit of CI was obtained from Sigma (Sigma Aldrich, Stockholm, Sweden) and the antibody directed to Tim23 (611223) was from BD Biosciences (Becton, Dickinson New Jersey USA). The HRP-coupled goat anti-mouse antibody (DAKO, Denmark A/S) was used for detection of primary antibodies.

3. Results

3.1. CIII activity in myxothiazol-exposed mice

The inhibitory effect of myxothiazol was investigated by CIII activity measurements from mitochondria isolated from livers of myxothiazol-exposed and control mice. In mice injected with myxothiazol, liver CIII activity decreased to 50% of control levels at 2 h post-injection (Fig. 1). The CIII activity recovered to a level of 80–100% of control value 24 h after the injection at all measured time points (24, 48, and 72 h). There were no overt signs of behavioral changes in the treated mice.

3.2. Liver histology

To assess the effect of myxothiazol administration on liver histology, basic histopathological analysis of the exposed animals was performed. Mild abnormalities were observed in HE-stained sections (Fig. 2), such as zonal cytoplasmic swelling and signs of regeneration (mitotic hepatocytes). Periodic acid-Schiff and diastase stainings did not reveal obvious changes in glycogen content upon myxothiazol administration.

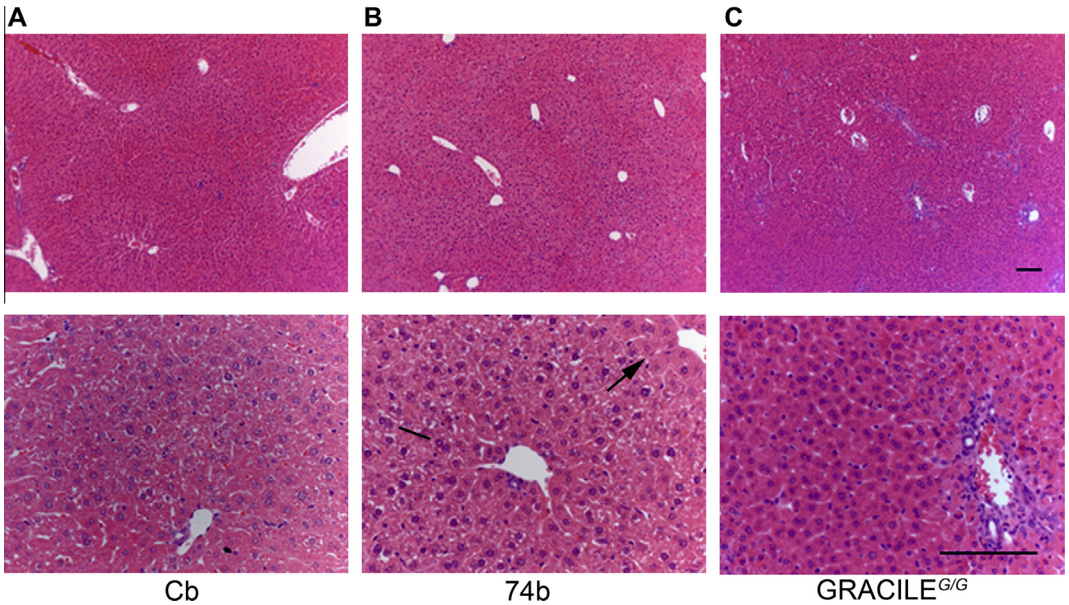

Fig. 2. Liver histology in myxothiazol-injected mice. (A) HE staining of liver from sham-exposed mouse shows normal architecture. (B) Staining of liver from mouse with CIII inhibition by 4 doses of myxothiazol shows zonal mild cytoplasmic swelling (paler areas, arrow) and pycnotic cells in the darker eosinophilic areas. Increased numbers of cells with double nuclei suggest regeneration (bar). (C) As a comparison, a liver section from a CIII deficient homozygous *BCS1L* mutant mouse (GRACILE$^{G/G}$) shows signs of advanced hepatopathy with steatosis and fibrosis. Scale bar is 10 μm.

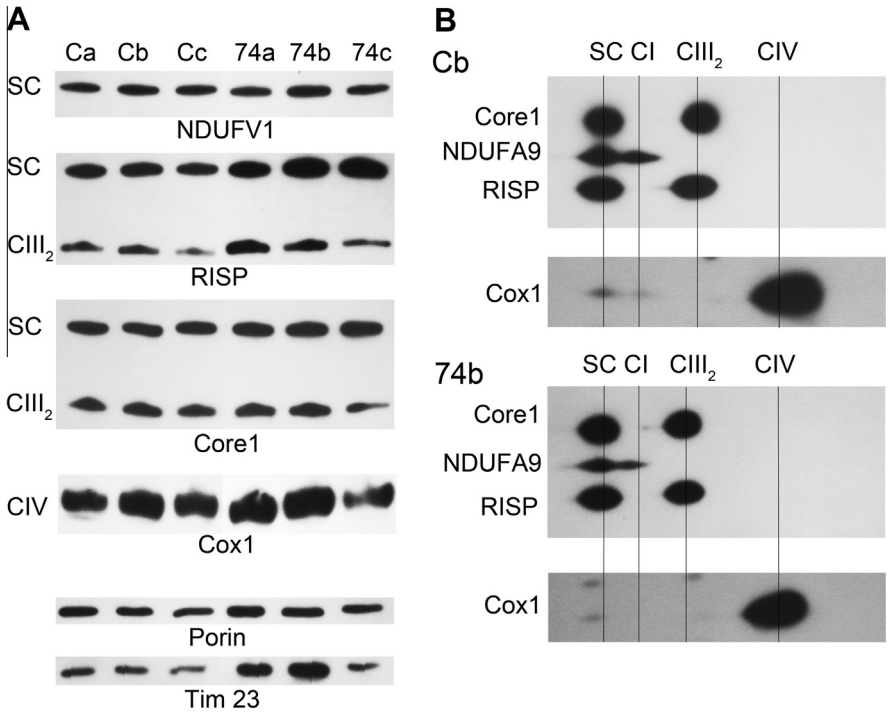

Fig. 3. Respiratory chain supercomplex assembly in liver mitochondria. (A) Inner membrane complexes separated with BNGE from isolated mitochondria of three (Ca–Cc) sham-treated animals and three (74a–74c) animals exposed to myxothiazol for 74 h. Porin and Tim23 were used as loading controls. (B) Mitochondrial complexes run with BNGE for first dimension and thereafter strips run on SDS–PAGE for the second dimension of one control (Cb) and one myxothiazol-exposed (74b) mouse. SC, supercomplex, CI, complex I, $CIII_2$, dimer of complex III, CIV, complex IV, RISP, Rieske iron-sulfur protein.

3.3. Triglyceride quantitation

Respiratory chain dysfunction can lead to microvesicular fat accumulation in hepatocytes by decreasing β-oxidation capacity [23]. To assess if myxothiazol administration causes changes in hepatic lipids, total triglyceride levels were measured in liver biopsies. There was no difference in the lipid content between mice given four doses of myxothiazol and sham treated animals (0.94–1.42 μg/mg vs 1.12–1.32 μg/mg), indicating that the duration and level of CIII inhibition achieved in this experiment did not cause signs of steatosis.

3.4. Respiratory chain supercomplex formation in myxothiazol-exposed mice

As supercomplex formation is a dynamic process influenced by the availability of assembly factors [24] as well as by structural changes in complexes [25], we wanted to investigate if the reversible CIII activity decrease induced by myxothiazol had an effect on supercomplex formation. BNGE analyses of isolated mitochondria showed similar assembly of CIII and supercomplex formation as in sham treated control animals (Fig. 3) after maximal exposure to myxothiazol, i.e. at 74 h after the first injection.

3.5. Effect of myxothiazol on liver gene expression

To investigate if CIII inhibition by myxothiazol could lead to changes in expression of CIII components or genes associated with hepatotoxicity, we extracted RNA from the livers obtained at 74 h and performed qPCR analyses. The expression levels of several of these genes were slightly downregulated in myxothiazol-exposed livers, but none of the changes were statistically significant. For example, the relative expression levels of the CIII-related genes *Risp*, *Uqcrc1* and *Bcs1l* were 0.65-fold to 0.70-fold in myxothiazol-exposed livers as compared with control values. Genes associated with hepatotoxicity, *Pygl* (1.20-fold) *Txnrd1* (0.71-fold), *Fmo1* (0.61-fold) and *Abcb11*/*Bsep* (0.73-fold) or inflammation *Tgf*-β (0.70-fold) were not changed significantly, either.

4. Discussion

We set out to develop an *in vivo* model of respiratory chain CIII deficiency. Using our injection regime adapted from a previous study [6], we found a reversible decrease of up to 50% in CIII activity in liver mitochondria of myxothiazol-exposed mice. The activity reverted to a level of more than eighty percent of baseline by 24 h after each of the repeated injections. The remaining 50% of CIII activity after drug administration seemed to be sufficient to maintain a respiratory chain function required for basal energy demand. At least no overt behavioral changes were observed in the mice. In addition, histological analysis revealed only minor changes in hepatocytes with preserved glycogen content. We found no signs of abnormal lipid accumulation in hepatocytes suggesting that short-term CIII inhibition is not sufficient to induce hepatic lipid accumulation. Furthermore, as no significant signs of hepatotoxicity were observed in histological or gene expression analyses, we consider the selected dosage safe for inducing experimental CIII deficiency *in vivo*. In a study on isolated rat hepatocytes, 50% inhibition by myxothiazol was needed to cause a major decrease in respiration [26].

Liver deterioration in *BCS1L* mutant mice becomes histologically detectable when the RISP content in CIII and activity have decreased to 50%. Thereafter, the progressive hepatopathy is rapid leading to end stage disorder within about one week [18]. Data from this genetic model and from pharmacological models suggest that in liver mitochondria CIII activity level of about 50% marks the threshold for onset of dysfunction. The first sign of CIII disturbance in the *BCS1L* mutant mice is microvesicular accumulation of lipids

in the hepatocytes [18]. Similar liver fat accumulation was also found in mice with a chemical liver-specific knockout of the Cox10 subunit of CIV [23]. In a study on mouse preadipocytes, respiratory chain inhibitors myxothiazol, stigmatellin and antimycin A caused triglyceride accumulation in a time- and concentration-dependent manner [27].

In the livers of *BCS1L* mutant mice, the RISP incorporation defect results in altered stoichiometry of CIII in respiratory chain supercomplexes, with both assembled CIII and precomplex CIII participating in supercomplex formation [25]. Thus, compensation mechanisms can be induced in the case of an assembly defect. This finding is also supported by the fact that in respirometry analyses of mutant mouse liver mitochondria a respiration defect was only seen at maximal capacity [18]. In the present study, we did not find any structural changes in CIII or in supercomplex formation after myxothiazol administration, suggesting a normal interaction between complexes I and III under these conditions.

We did not find any significant changes in the mRNA levels of assembly factors, nor in inflammation or toxicity markers in myxothiazol-injected mice. Thus, the short-term chemical inhibition of CIII did not result in any signs of compensatory regulation. These findings are in line with the minor histological changes observed in the myxothiazol-exposed livers.

Neither did we find any signs of inflammation in the liver exposed to myxothiazol. However, the sensitivity to dysfunction in respiratory chain complexes is highly variable in different tissues [13,26,28].

Recently, in a systematic *in vivo* study using the zebrafish model, inhibitors of all respiratory chain complexes were used to investigate developmental effects of respiratory chain inhibition. The goal of the study was to develop a model for testing mitochondria-targeted drugs [29]. In the zebrafish model, myxothiazol caused severe mitochondrial dysfunction and embryonic lethality. Inhibition of CI and CII resulted in less severe phenotypes, suggesting active alternative pathways for electron feeding to CIII [29]. Thus, to biochemically induce mitochondrial dysfunction, targeting CIII seems to be an efficient strategy.

In conclusion, with our myxothiazol administration protocol we achieved acute and reversible CIII inhibition that after a course of four days showed no overt adverse effects in mice. This biochemical *in vivo* model of acute respiratory chain inhibition could be utilized in future studies of new therapies targeting mitochondria.

Acknowledgments

The study was supported by Grants from Swedish Research Council (VF), governmental ALF research grants to Lund University and Lund University Hospital (VF), Finnish Academy (VF), Sigrid Juselius Foundation (PL), Finnish Cultural Foundation (SM), Foundation for Pediatric Research in Finland (VF), and Finnish Physicians' Society (VF). We gratefully acknowledge Professor Rolf Muller, Helmholtz-Center for Infection Research, Braunschweig Germany for providing us with myxothiazol, Associate professor Matti Jauhiainen for triglyceride assessments, and technician Tuula Manninen for performing CIII activity measurements.

References

[1] L. Esser, B. Quinn, Y.F. Li, M. Zhang, M. Elberry, L. Yu, C.A. Yu, D. Xia, Crystallographic studies of quinol oxidation site inhibitors: a modified classification of inhibitors for the cytochrome *bc*(1) complex, J. Mol. Biol. 341 (2004) 281–302.

[2] T. Tron, M. Crimi, A.M. Colson, M. Degli, Esposti, structure/function relationships in mitochondrial cytochrome *b* revealed by the kinetic and circular dichroic properties of two yeast inhibitor-resistant mutants, Eur. J. Biochem. 199 (1991) 753–760.

[3] K. Gerth, H. Irschik, H. Reichenbach, W. Trowitzsch, Myxothiazol, an antibiotic from *Myxococcus fulvus* (myxobacterales). I. Cultivation, isolation, physicochemical and biological properties, J. Antibiot. 33 (1980) 1474–1479.

[4] G. von Jagow, W.D. Engel, Complete inhibition of electron transfer from ubiquinol to cytochrome *b* by the combined action of antimycin and myxothiazol, FEBS Lett. 136 (1981) 19–24.

[5] T.A. Young, C.C. Cunningham, S.M. Bailey, Reactive oxygen species production by the mitochondrial respiratory chain in isolated rat hepatocytes and liver mitochondria: studies using myxothiazol, Arch. Biochem. Biophys. 405 (2002) 65–72.

[6] J.W. Zmijewski, E. Lorne, S. Banerjee, E. Abraham, Participation of mitochondrial respiratory complex III in neutrophil activation and lung injury, Am. J. Physiol. Lung Cell. Mol. Physiol. 296 (2009) L624–L634.

[7] C. Nogueira, J. Barros, M.J. Sa, L. Azevedo, R. Taipa, A. Torraco, M.C. Meschini, D. Verrigni, C. Nesti, T. Rizza, J. Teixeira, R. Carrozzo, M.M. Pires, L. Vilarinho, F.M. Santorelli, Novel TTC19 mutation in a family with severe psychiatric manifestations and complex III deficiency, Neurogenetics 14 (2013) 153–160.

[8] D. Ghezzi, P. Arzuffi, M. Zordan, C. Da Re, C. Lamperti, C. Benna, P. D'Adamo, D. Diodato, R. Costa, C. Mariotti, G. Uziel, C. Smiderle, M. Zeviani, Mutations in TTC19 cause mitochondrial complex III deficiency and neurological impairment in humans and flies, Nat. Genet. 43 (2011) 259–263.

[9] E.J. Tucker, B.F. Wanschers, R. Szklarczyk, H.S. Mountford, X.W. Wijeyeratne, M.A. van den Brand, A.M. Leenders, R.J. Rodenburg, B. Reljic, A.G. Compton, A.E. Frazier, D.L. Bruno, J. Christodoulou, H. Endo, M.T. Ryan, L.G. Nijtmans, M.A. Huynen, D.R. Thorburn, Mutations in the UQCC1-interacting protein, UQCC2 cause human complex III deficiency associated with perturbed cytochrome *b* protein expression, PLoS Genet. 9 (2013) e1004034.

[10] V. Fellman, H. Kotarsky, Mitochondrial hepatopathies in the newborn period, Semin. Fetal. Neonatal. Med. 16 (2011) 222–228.

[11] P. de Lonlay, I. Valnot, A. Barrientos, M. Gorbatyuk, A. Tzagoloff, J.W. Taanman, E. Benayoun, D. Chretien, N. Kadhom, A. Lombes, H.O. de Baulny, P. Niaudet, A. Munnich, P. Rustin, A. Rotig, A mutant mitochondrial respiratory chain assembly protein causes complex III deficiency in patients with tubulopathy, encephalopathy and liver failure, Nat. Genet. 29 (2001) 57–60.

[12] E. Fernandez-Vizarra, M. Bugiani, P. Goffrini, F. Carrara, L. Farina, E. Procopio, A. Donati, G. Uziel, I. Ferrero, M. Zeviani, Impaired complex III assembly associated with *BCS1L* gene mutations in isolated mitochondrial encephalopathy, Hum. Mol. Genet. 16 (2007) 1241–1252.

[13] D. Spitkovsky, P. Sasse, E. Kolossov, C. Bottinger, B.K. Fleischmann, J. Hescheler, R.J. Wiesner, Activity of complex III of the mitochondrial electron transport chain is essential for early heart muscle cell differentiation, FASEB J. 18 (2004) 1300–1302.

[14] H. Kotarsky, M. Keller, M. Davoudi, P. Leveen, R. Karikoski, D.P. Enot, V. Fellman, Metabolite profiles reveal energy failure and impaired beta-oxidation in liver of mice with complex III deficiency due to a *BCS1L* mutation, PLoS ONE 7 (2012) e41156.

[15] V. Fellman, S. Lemmela, A. Sajantila, H. Pihko, I. Jarvela, Screening of *BCS1L* mutations in severe neonatal disorders suspicious for mitochondrial cause, J. Hum. Genet. 53 (2008) 554–558.

[16] I. Visapaa, V. Fellman, J. Vesa, A. Dasvarma, J.L. Hutton, V. Kumar, G.S. Payne, M. Makarow, R. Van Coster, R.W. Taylor, D.M. Turnbull, A. Suomalainen, L. Peltonen, GRACILE syndrome, a lethal metabolic disorder with iron overload, is caused by a point mutation in *BCS1L*, Am. J. Hum. Genet. 71 (2002) 863–876.

[17] V. Fellman, J. Rapola, H. Pihko, T. Varilo, K.O. Raivio, Iron-overload disease in infants involving fetal growth retardation, lactic acidosis, liver haemosiderosis, and aminoaciduria, Lancet 351 (1998) 490–493.

[18] P. Leveen, H. Kotarsky, M. Morgelin, R. Karikoski, E. Elmer, V. Fellman, The GRACILE mutation introduced into Bcs1l causes postnatal complex III deficiency: a viable mouse model for mitochondrial hepatopathy, Hepatology 53 (2011) 437–447.

[19] J. Folch, M. Lees, G.H. Sloane, Stanley, A simple method for the isolation and purification of total lipides from animal tissues, J. Biol. Chem. 226 (1957) 497–509.

[20] N. Zidek, J. Hellmann, P.J. Kramer, P.G. Hewitt, Acute hepatotoxicity: a predictive model based on focused illumina microarrays, Toxicol. Sci. 99 (2007) 289–302.

[21] P. Burra, D. Arcidiacono, D. Bizzaro, T. Chioato, R. Di Liddo, A. Banerjee, A. Cappon, P. Bo, M.T. Conconi, P.P. Parnigotto, S. Mirandola, E. Gringeri, A. Carraro, U. Cillo, F.P. Russo, Systemic administration of a novel human umbilical cord mesenchymal stem cells population accelerates the resolution of acute liver injury, BMC Gastroenterol. 12 (2012) 88.

[22] H. Schagger, W.A. Cramer, G. von Jagow, Analysis of molecular masses and oligomeric states of protein complexes by blue native electrophoresis and isolation of membrane protein complexes by two-dimensional native electrophoresis, Anal. Biochem. 217 (1994) 220–230.

[23] F. Diaz, S. Garcia, D. Hernandez, A. Regev, A. Rebelo, J. Oca-Cossio, C.T. Moraes, Pathophysiology and fate of hepatocytes in a mouse model of mitochondrial hepatopathies, Gut 57 (2008) 232–242.

[24] E. Lapuente-Brun, R. Moreno-Loshuertos, R. Acin-Perez, A. Latorre-Pellicer, C. Colas, E. Balsa, E. Perales-Clemente, P.M. Quiros, E. Calvo, M.A. Rodriguez-Hernandez, P. Navas, R. Cruz, A. Carracedo, C. Lopez-Otin, A. Perez-Martos, P. Fernandez-Silva, E. Fernandez-Vizarra, J.A. Enriquez, Supercomplex assembly determines electron flux in the mitochondrial electron transport chain, Science 340 (2013) 1567–1570.

[25] M. Davoudi, H. Kotarsky, E. Hansson, V. Fellman, Complex I function and supercomplex formation are preserved in liver mitochondria despite progressive complex III deficiency, PLoS ONE 9 (2014) e86767.
[26] R.W. Taylor, M.A. Birch-Machin, K. Bartlett, S.A. Lowerson, D.M. Turnbull, The control of mitochondrial oxidations by complex III in rat muscle and liver mitochondria. Implications for our understanding of mitochondrial cytopathies in man, J. Biol. Chem. 269 (1994) 3523–3528.
[27] S. Vankoningsloo, M. Piens, C. Lecocq, A. Gilson, A. De Pauw, P. Renard, C. Demazy, A. Houbion, M. Raes, T. Arnould, Mitochondrial dysfunction induces triglyceride accumulation in 3T3-L1 cells: role of fatty acid beta-oxidation and glucose, J. Lipid Res. 46 (2005) 1133–1149.
[28] A.S. Midzak, J. Liu, B.R. Zirkin, H. Chen, Effect of myxothiazol on Leydig cell steroidogenesis: inhibition of luteinizing hormone-mediated testosterone synthesis but stimulation of basal steroidogenesis, Endocrinology 148 (2007) 2583–2590.
[29] B.R. Pinho, M.M. Santos, A. Fonseca-Silva, P. Valentao, P.B. Andrade, J.M. Oliveira, How mitochondrial dysfunction affects zebrafish development and cardiovascular function: an in vivo model for testing mitochondria-targeted drugs, Br. J. Pharmacol. 169 (2013) 1072–1090.